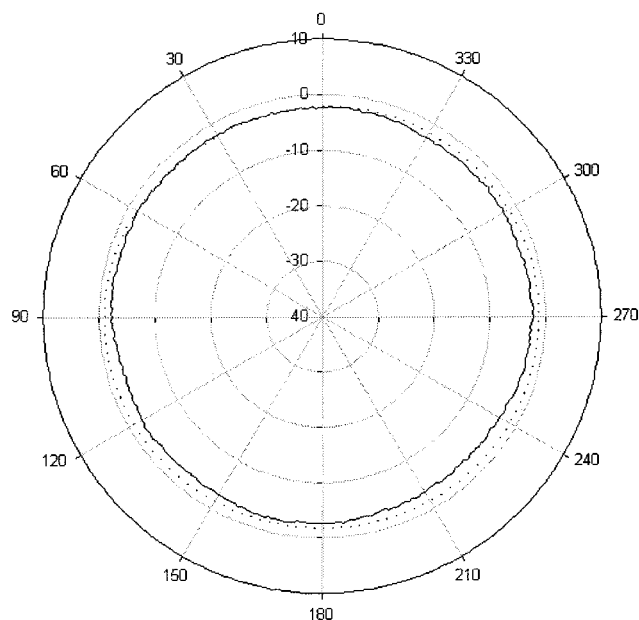


(a)



(b)

Figure 3 Radiation pattern at 2.44 GHz (solid: measurement, dotted: simulation) (a) xz plane, (b) xy plane

that of a monopole antenna. The patch of this antenna is used to match the impedance, therefore it has nothing to do with the radiation pattern. The size of the ground plane is $15 \text{ cm} \times 15 \text{ cm}$. The calculated and measured antenna gains in the xz plane have 2.92 and 2.73 dBi, respectively. This slight discrepancy can be attributed to the effects of the finite ground plane and conductor loss. The gain of the proposed antenna is higher than that of a similar-size antenna [3].

4. CONCLUSIONS

The proposed antenna has a small size and high gain that was verified with measurement and simulation. As seen in Figure 2, the resonant frequency of the present model can be reduced by 35% compared to the conventional antenna. Impedance bandwidth (VSWR < 2) and gain have 9.0% and 2.73 dBi, respectively. Although the size of the proposed antenna is similar to that of a chip antenna, the gain of the antenna is higher than that of a chip antenna [4]. This has a useful application for the ISM band (2.4–2.4835 GHz).

REFERENCES

1. M. Ali and S.S. Stuchly, A meander-line bow-tie antenna, *Antennas Propagat Soc Int Symp 3* (1996), 1566–1569.
2. M. Ali, S.S. Stuchly, and K. Caputa, A wideband dual meander sleeve antenna, *Antennas Propagat Soc Int Symp 3* (1996), 1598–1601.
3. M. Chair, K.M. Luk, and K.F. Lee, Miniature multilayer shorted patch antenna, *Electron Lett 36* (2000), pp 3 and 4.
4. Y. Dakeya, T. Suesada, K. Asakura, N. Nakajima, and H. Mandai, Chip multilayer antenna for 2.45 GHz-Band Application using LTCC technology, *IEEE MTT-S Int 3* (2000), 1693–1696.

© 2002 Wiley Periodicals, Inc.

AN IMPEDANCE BOUNDARY CONDITION FOR THE EFFICIENT MATCHED TERMINATION OF WAVEGUIDES IN FDTD SIMULATIONS

José A. Pereda, Ángel Vegas, Andrés Prieto, and Oscar Caño

Departamento de Ingeniería de Comunicaciones (DICOM)
Universidad de Cantabria
Avda. Los Castros s/n
39005 Santander, Spain

Received 18 January 2002

ABSTRACT: This Letter introduces a novel impedance boundary condition (IBC) for the matched termination of waveguide ports in finite-difference–time-domain (FDTD) simulators. It is based on approximating the wave impedance by a rational function over the frequency band of interest. To show the validity of the proposed IBC, the reflection coefficient of a wideband matched 90° H-plane corner in rectangular waveguide is computed. The results obtained, which are less than -45 dB over the whole waveguide band, are in good agreement with those obtained by a commercial finite-element simulator. © 2002 Wiley Periodicals, Inc. *Microwave Opt Technol Lett 34*: 151–155, 2002; Published online in Wiley InterScience (www.interscience.wiley.com). DOI 10.1002/mop.10400

Key words: FDTD methods; impedance boundary condition; waveguide

1. INTRODUCTION

The finite-difference–time-domain (FDTD) method is a powerful and flexible technique for the analysis of a great variety of electromagnetic problems. Applying the FDTD method to the computation of scattering parameters of microwave circuits requires an adequate termination of the circuit ports. This usually means that reflected waves should be eliminated by properly matching the ports.

The accurate and efficient wideband matching of waveguide ports is therefore an interesting topic that has received considerable attention over the last few years. The approaches available, for the matched termination of waveguides in FDTD simulations

can be grouped into three main categories: the use of one-way absorbing boundary conditions (one-way ABCs) [1, 2], perfect matched layers [3, 4], and impedance boundary conditions (IBCs) [5, 6].

The application of IBCs to the matching of waveguide ports basically consists of terminating the waveguide by an impedance with the same value as the wave impedance of the mode under consideration. The wave impedance is then implemented, at the waveguide terminal plane, by relating the appropriate transverse field components.

Unfortunately, wave impedance is not a rational function of frequency. Consequently, the exact relation between fields and wave impedance can not be written as a differential equation in the time domain. In spite of this, IBCs can still be implemented in various *exact* or approximate, ways. Analytically exact IBCs have been derived by expressing the impedance relation as a convolution product in the time domain [5]. This approach, however, leads to computationally expensive global-in-time algorithms. Several authors have tried to alleviate this drawback by procedures such as windowing the convolved functions [6], or modeling boundary conditions as digital filters [7]. These procedures, which are used to obtain approximate but more efficient IBCs, have the common characteristic that they are applied in the time domain.

This Letter presents a novel and efficient IBC based on approximating the wave impedance by a rational function of the frequency. This approximation is carried out in the frequency domain, which has the advantage of minimizing the approximation error in the frequency band of interest. As a consequence, the efficiency of the resulting IBC is greater than that obtained by using approximation techniques carried out in the time domain.

To validate this IBC, the computation of the reflection coefficient of a wideband matched 90° *H*-plane corner in a rectangular waveguide. As will be shown, this structure presents a reflection coefficient of less than -45 dB over the whole waveguide band, and therefore the good performance of the IBC used in this example is of great importance. The results obtained have been compared with those given by the HFSS commercial finite-element simulator.

2. THEORY

Approximation of the Exact IBC. To illustrate the development of the proposed IBC, a rectangular waveguide propagating the dominant TE₁₀ mode in the positive *z* direction will be considered. In order to terminate the waveguide at the plane $z = z_{\max}$, consider the expression

$$E_y(s) = -Z_\omega(s)H_x(s), \quad (1)$$

which relates, in the Laplace domain, the transverse field components through the wave impedance of the TE₁₀ mode:

$$Z_\omega(s) = \frac{\eta s}{\sqrt{s^2 + (\pi/a)^2}},$$

where η is the intrinsic impedance and a is the waveguide width.

The first step consists of approximating, in the frequency band of interest, the wave impedance by a second-order rational function

$$Z_\omega(s) \approx \frac{a_0 + a_1s + a_2s^2}{1 + b_1s + b_2s^2},$$

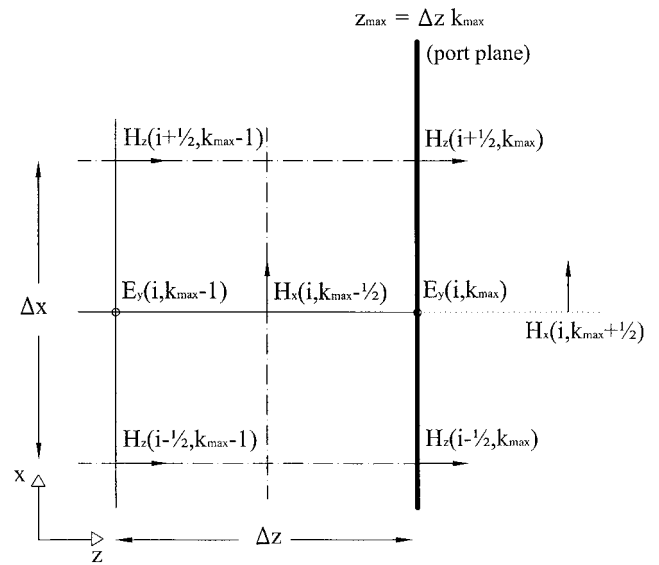


Figure 1 FDTD cell in the neighborhood of a waveguide port

where a_m and b_m are real-value coefficients. Then (1) can be approximated by

$$E_y(s) = -\frac{a_0 + a_1s + a_2s^2}{1 + b_1s + b_2s^2} H_x(s), \quad (2)$$

which constitutes an approximated IBC expressed in the Laplace domain.

Discretization of the Approximated IBC. Now discrete-time version of (2) that would be consistent with the conventional FDTD equations must be derived to solve the fields in the interior of the waveguide. The strategy followed to attain this goal consists of first applying the Mobius transformation

$$s = \frac{2}{\Delta_t} \frac{1 - Z^{-1}}{1 + Z^{-1}}, \quad (3)$$

to transform (2) into the *Z*-transform domain as

$$E_y(Z) = -\frac{c_0 + c_1Z^{-1} + c_2Z^{-2}}{1 + d_1Z^{-1} + d_2Z^{-2}} H_x(Z),$$

where the coefficients c_m and d_m are related to a_m and b_m , and to the time step Δ_t . This equation is then written in difference form by simply considering the relationship $Z^{-m}F(Z) \leftrightarrow F^{n-m}$, which leads to

$$E_y^{n+1}(\mathbf{r}_{E_y}) + \sum_{m=1}^2 d_m E_y^{n-m+1}(\mathbf{r}_{E_y}) = -\sum_{m=0}^2 c_m H_x^{n-m+1}(\mathbf{r}_{E_y}), \quad (4)$$

where field quantities are evaluated at an arbitrary E_y node of the waveguide port. This node, which is shown in Figure 1, is denoted as

$$\mathbf{r}_{E_y} = i \Delta_x \hat{x} + k_{\max} \Delta_z \hat{z} \equiv (i, k_{\max}).$$

To reduce memory requirements, (4) is rewritten as an equivalent set of first-order difference equations. This can easily be done

by using digital filtering techniques such as the transpose direct method II [8], which leads to

$$\begin{aligned} E_y^{n+1/2}(\mathbf{r}_{E_y}) &= W_1^{n-1/2}(\mathbf{r}_{E_y}) - c_0 H_x^{n+1/2}(\mathbf{r}_{E_y}), \\ W_1^{n+1/2}(\mathbf{r}_{E_y}) &= W_2^{n-1/2}(\mathbf{r}_{E_y}) - d_1 E_y^{n+1/2}(\mathbf{r}_{E_y}) - c_1 H_x^{n+1/2}(\mathbf{r}_{E_y}), \\ W_2^{n+1/2}(\mathbf{r}_{E_y}) &= -c_2 H_x^{n+1/2}(\mathbf{r}_{E_y}) - d_2 E_y^{n+1/2}(\mathbf{r}_{E_y}), \end{aligned} \quad (5)$$

where W_1 and W_2 are auxiliary variables.

The discretization procedure described in this section has been successfully employed in other areas of FDTD research, for example, in the incorporation of dispersive media into FDTD simulators [9].

Synchronization with the Conventional FDTD Scheme. Notice that in the set of equations (5), E_y is evaluated at time instants $t = (n + 1/2) \Delta_t$ and H_x at spatial points $z_{\max} = k_{\max} \Delta_z$. As a consequence, these equations can not be directly implemented because, as is shown in Figure 1, the conventional FDTD scheme evaluates E_y at time instants $t = n \Delta_t$ and H_x at spatial points $z = (k + 1/2) \Delta_z$. To overcome this problem, the average in time is used to evaluate $E_y^{n+1/2}(\mathbf{r}_{E_y})$ as

$$E_y^{n+1/2}(\mathbf{r}_{E_y}) \approx \frac{1}{2} [E_y^n(\mathbf{r}_{E_y}) + E_y^{n+1}(\mathbf{r}_{E_y})], \quad (6)$$

and the average in space to evaluate $H_x^{n+1/2}(\mathbf{r}_{E_y})$ as

$$H_x^{n+1/2}(\mathbf{r}_{E_y}) \approx \frac{1}{2} \left[H_x^{n+1/2} \left(\mathbf{r}_{E_y} + \frac{\Delta_z}{2} \hat{z} \right) + H_x^{n+1/2} \left(\mathbf{r}_{E_y} - \frac{\Delta_z}{2} \hat{z} \right) \right]. \quad (7)$$

This approach, however, introduces the field $H_x^{n+1/2}(\mathbf{r}_{E_y} + (\Delta_z/2)\hat{z})$, which is defined at a spatial position that is outside of the problem region, as is also illustrated in Figure 1. A new equation must then be added to compensate for this new unknown. For this purpose the Ampère-Maxwell equation discretized according to the conventional FDTD scheme is used:

$$\begin{aligned} E_y^{n+1}(\mathbf{r}_{E_y}) &= E_y^n(\mathbf{r}_{E_y}) + \frac{\Delta_t}{\Delta_z \epsilon} \left[H_x^{n+1/2} \left(\mathbf{r}_{E_y} + \frac{\Delta_z}{2} \hat{z} \right) \right. \\ &\quad \left. - H_x^{n+1/2} \left(\mathbf{r}_{E_y} - \frac{\Delta_z}{2} \hat{z} \right) \right] - \frac{\Delta_t}{\Delta_x \epsilon} \left[H_z^{n+1/2} \left(\mathbf{r}_{E_y} + \frac{\Delta_x}{2} \hat{x} \right) \right. \\ &\quad \left. - H_z^{n+1/2} \left(\mathbf{r}_{E_y} - \frac{\Delta_x}{2} \hat{x} \right) \right]. \end{aligned} \quad (8)$$

Now solving equations (5)–(8) for the fields that are more advanced in time leads to

$$\begin{aligned} E_y^{n+1}(\mathbf{r}_{E_y}) &= \frac{c_0 \Delta_z \epsilon / \Delta_t - 1}{c_0 \Delta_z \epsilon / \Delta_t + 1} E_y^n(\mathbf{r}_{E_y}) + \frac{2}{c_0 \Delta_z \epsilon / \Delta_t + 1} \\ &\quad \times \left[W_1^{n-1/2}(\mathbf{r}_{E_y}) - c_0 H_x^{n+1/2} \left(\mathbf{r}_{E_y} - \frac{\Delta_z}{2} \hat{z} \right) \right] \\ &\quad - \frac{\Delta_z c_0 / \Delta_x}{c_0 \Delta_z \epsilon / \Delta_t + 1} \left[H_z^{n+1/2} \left(\mathbf{r}_{E_y} + \frac{\Delta_x}{2} \hat{x} \right) - H_z^{n+1/2} \left(\mathbf{r}_{E_y} - \frac{\Delta_x}{2} \hat{x} \right) \right], \\ E_y^{n+1/2}(\mathbf{r}_{E_y}) &= \frac{1}{2} [E_y^n(\mathbf{r}_{E_y}) + E_y^{n+1}(\mathbf{r}_{E_y})], \end{aligned}$$

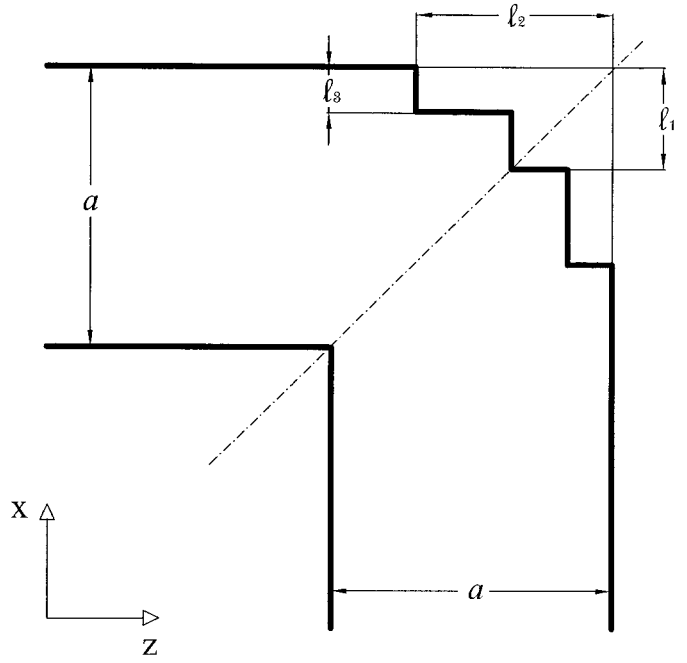


Figure 2 Wideband matched 90° H -plane corner in rectangular waveguide. Distances are given in the text

$$\begin{aligned} H_x^{n+1/2} \left(\mathbf{r}_{E_y} + \frac{\Delta_z}{2} \hat{z} \right) &= \frac{2}{c_0} [W_1^{n-1/2}(\mathbf{r}_{E_y}) - E_y^{n+1/2}(\mathbf{r}_{E_y})] - H_x^{n+1/2} \left(\mathbf{r}_{E_y} - \frac{\Delta_z}{2} \hat{z} \right), \\ H_x^{n+1/2}(\mathbf{r}_{E_y}) &= \frac{1}{2} \left[H_x^{n+1/2} \left(\mathbf{r}_{E_y} - \frac{\Delta_z}{2} \hat{z} \right) + H_x^{n+1/2} \left(\mathbf{r}_{E_y} + \frac{\Delta_z}{2} \hat{z} \right) \right], \\ W_1^{n+1/2}(\mathbf{r}_{E_y}) &= W_2^{n-1/2}(\mathbf{r}_{E_y}) - d_1 E_y^{n+1/2}(\mathbf{r}_{E_y}) - c_1 H_x^{n+1/2}(\mathbf{r}_{E_y}), \\ W_2^{n+1/2}(\mathbf{r}_{E_y}) &= -c_2 H_x^{n+1/2}(\mathbf{r}_{E_y}) - d_2 E_y^{n+1/2}(\mathbf{r}_{E_y}). \end{aligned}$$

This set of equations is now ready to be directly implemented in an FDTD simulator. This IBC has a number of interesting properties: It is a formulation that preserves the second-order accuracy of the conventional FDTD scheme; it is properly synchronized in space and time (to be consistent with the conventional FDTD scheme); and it requires only three additional storage variables, $W_1(i, k_{\max})$, $W_2(i, k_{\max})$, and $H_x(i, k_{\max} + 1/2)$, per each E_y node located at the port.

3. VALIDATION

To validate the IBC presented in the previous section, the scattering parameters of a 90° H -plane corner in WR75 waveguide have been computed. In order to obtain good matching over the whole frequency band (10–15 GHz), the corner has been modified as shown in Figure 2. As will be shown, this arrangement provides a reflection coefficient of less than -45 dB over the entire frequency band.

To minimize numerical errors other than those due to the absorbing boundary conditions, the structure under analysis has been discretized by a very fine FDTD mesh of $\Delta_x = \Delta_z = \Delta =$

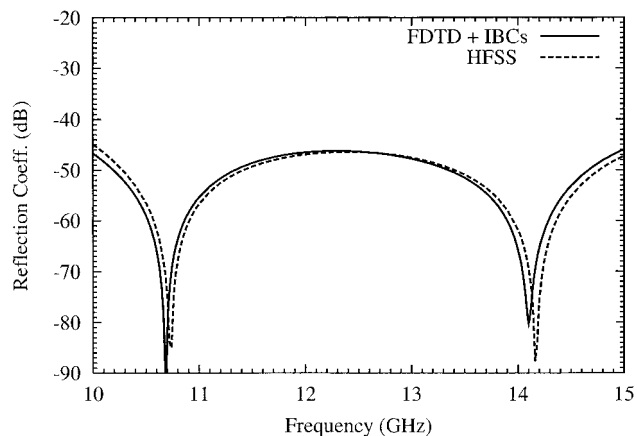


Figure 3 Reflection coefficient for the structure shown in Figure 2. Solid line, FDTD + proposed IBC; dashed line, HFSS

$a/198$. The other distances shown in Figure 2 are $l_1 = 72\Delta$, $l_2 = 140\Delta$, and $l_3 = 30\Delta$.

Figure 3 shows the modulus of the scattering parameter S_{11} computed by the FDTD method with both ports of the structure terminated by the IBC presented in the above section. In order to check the accuracy of these results, the data obtained by means of the HFSS commercial simulator are also plotted. Apart from a slight frequency shift, it can be seen that the results computed by the two methods are in good agreement.

The use of absorbing boundary conditions that are not sufficiently accurate in FDTD simulations may have a large impact on the numerical results obtained. To illustrate this idea we have recomputed the modulus of the scattering parameter S_{11} by the FDTD method. All the parameters, except the boundary conditions at the waveguide ports, have been held the same as in the previous FDTD simulation. In this case, both ports of the structure shown in Figure 2 have been terminated by a second-order one-way ABC in which phase speeds have been taken to be equal to the speed of light in free space (this condition is equivalent to a second-order ABC given in [10]). Figure 4 compares the results obtained for this second FDTD simulation with those provided by HFSS. It can be observed that, in this case, the FDTD results are so distorted that they are definitely not useful.

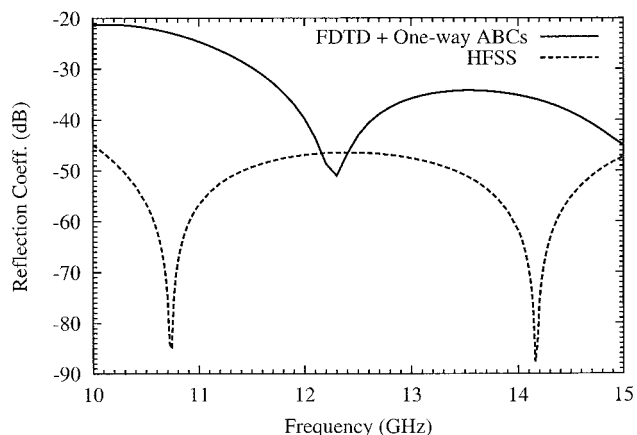


Figure 4 Reflection coefficient for the structure shown in Figure 2. Solid line, FDTD + one-way equation; dashed line, HFSS

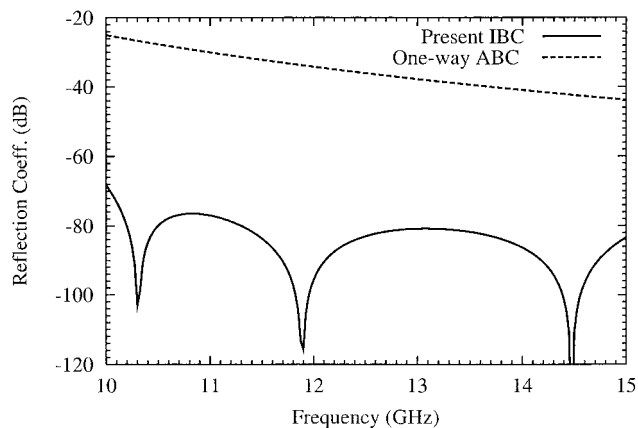


Figure 5 Spurious reflection coefficient presented by the proposed IBC (solid line) and by a one-way equation (dashed line)

Finally, to illustrate more precisely the performance of the proposed IBC the modulus of the reflection coefficient provided by this boundary condition when it is used to terminate a waveguide port has been computed. The parameters of the FDTD discretization are the same as in the simulations described previously. The results obtained are depicted in Figure 5, which shows that the reflection coefficient is below -70 dB over the whole frequency band. For the sake of comparison, Figure 5 also shows the reflection coefficient provided by the one-way ABC used to obtain the results shown in Figure 4. It can be seen that the performance of this boundary condition is very poor, which explains the bad results of Figure 4.

4. CONCLUSION

This Letter has introduced an IBC for the matched termination of waveguides. To develop this IBC, first the wave impedance is approximated, in the frequency band of interest, by a second-order rational function of the frequency. The resulting approximated impedance is then used to relate the appropriate electric and magnetic field components at the waveguide ports. The discretization of the IBC obtained in this way follows a procedure that combines the application of the Mobius transformation with the averaging of the electric and magnetic fields in time and space, respectively. This averaging is required to properly synchronize—in space and time—the IBC with the conventional FDTD scheme, while maintaining at the same time the second-order nature of the scheme.

To illustrate the validity of the IBC proposed, the computation of the reflection coefficient presented by a wideband matched 90° H -plane corner in rectangular waveguide was considered. The results obtained are in good agreement with those provided by HFSS. It has also been shown how the use of insufficiently accurate boundary conditions may have a dramatic impact on the results obtained.

REFERENCES

1. M. De Pourcq, Field and power-density calculations in closed microwave systems by three-dimensional finite differences, *IEE Proc Pt H* 132 (1985), 360–368.
2. L.A. Vielva, J.A. Pereda, A. Vegas, and A. Prieto, Multimode characterization of waveguide devices using absorbing boundary conditions for propagating and evanescent modes, *IEEE Microwave Guided Wave Lett MGW-4* (1994), 160–162.
3. C.E. Reuter, R.M. Joseph, E.T. Thiele, D.S. Katz, and A. Taflove, Ultrawideband absorbing boundary condition for termination of

- waveguiding structures in FD-TD simulations, *IEEE Microwave Guided Wave Lett MGW-4* (1994), 344–346.
4. K.Y. Jung, H. Kim, and K.C. Ko, A modified perfectly matched layers (PML) for waveguide problems, *Microwave Opt Technol Lett* 18 (1998), 360–362.
 5. F. Moglie, T. Rozzi, P. Marcozzi, and A. Schiavoni, A new termination condition for the application of FDTD techniques to discontinuity problems in close homogeneous waveguide, *IEEE Microwave Guided Wave Lett MGW-2* (1992), 475–477.
 6. F. Alimanti, P. Mezzanote, L. Roselli, and R. Sorrentino, Modal absorption in the FDTD method: A critical review, *Int J Numerical Modeling* 10 (1997), 245–264.
 7. A. Kreczkowski, T. Rutkowski, and M. Mrozowski, Fast modal ABC's in the hybrid PEE-FDTD analysis of waveguide discontinuities, *IEEE Microwave Guided Wave Lett MGW-9* (1999), 186–199.
 8. J.G. Proakis and D.G. Manolakis, *Digital signal processing. Principles, algorithms and applications*. Macmillan, New York, 1992.
 9. J.A. Pereda, A. Vegas, and A. Prieto, FDTD modeling of wave propagation in dispersive media by using the Mobius transformation technique, *IEEE Trans Microwave Theory Tech* (in press).
 10. G. Mur, Absorbing boundary conditions for the finite-difference approximation of the time-domain electromagnetic-field equations, *IEEE Trans Electromagn Compat EC-23* (1981), 377–382.

© 2002 Wiley Periodicals, Inc.